03

Modelling of a helical vortex dynamics based on the nonlinear Schrödinger equation

© P.A. Kuibin

Kutateladze Institute of Thermophysics, Siberian Branch, Russian Academy of Sciences, Novosibirsk, Russia
E-mail: pak0659@mail.ru

Received December 11, 2025
Revised January 22, 2026
Accepted January 23, 2026

The paper is devoted to the study of the dynamics of a conical helical vortex based on a known approach in which the equations of vortex motion within the framework of the local induction approximation are transformed into a nonlinear Schrödinger equation. A conical helical vortex, similar to that observed in experiments, was considered as the initial configuration. Numerical calculations revealed the development of the wave structure and the emergence of conditions preceding vortex reconnection. The results may be utilized to predict the operational regimes of a hydraulic turbine characterized by aperiodic strong pressure pulses in the hydraulic turbine's circuit.

Keywords: vortex, local induction approximation, nonlinear Schrödinger equation, numerical simulation.

DOI: 10.61011/TPL.2026.05.63291.20598

Vortex flows often occur in nature and are widely used in engineering. Swirling is used to intensify and stabilize heat and mass transfer processes, improve combustion and impurity separation, etc. At the same time, vortex initiation can also cause negative effects. Thus, a large-scale vortex rope can occur in a hydraulic turbine, causing heavy pressure surges. Simulated experiments performed earlier at the Institute of Thermophysics, Siberian Branch, Russian Academy of Sciences, have detected an interesting type of helical vortex instability where the neighboring turns of the helical vortex came closer together and got reconnected afterwards to form a vortex ring [1]. A local induction approximation (LIA) method is distinguished as the most cost-effective among the methods for numerical simulation of vortex filament dynamics. As reported in [2], LIA was proposed by Da Rios in 1906 [3], and later LIA was again proposed in [4–6]. A transformation found in [7] has become an important milestone in the approach evolution and allowed switching from the local induction equation (LIE) to the nonlinear Schrödinger equation (NSE). Thus, a solution for a soliton traveling on a vortex line has been obtained. A two-soliton solution was later found in [8] and a N-soliton solution was found in [9]. Another class of NSE solutions represents so called breather solutions (see [10] and references therein), which, unlike solitons, are localized perturbations. A breather solution that gives a classical helical vortex within $t \to \pm\infty$ is discussed in [10]. Having taken a breather solution at $t = -800$ (perturbed helical vortex) as an initial condition, the author examined the helical vortex behavior both through solution of LIE and directly on the basis of Biot–Savart's law. It is impossible to calculate reconnection using LIA, however, it has been established in [10] that the LIA method could be used to predict the behavior that precedes reconnection. And transition to NSE makes it possible to solve the problem in curvature–torsion variables, which are an excellent indicator of a pre-reconnection configuration. Unlike the perturbed classical helical vortex [10], a conical helical vortex occurs in the experiment [1] just as in a real hydraulic turbine and is prone to inherent instability. It is the NSE solution for the conical helical vortex that is proposed in this work.

In LIA, velocity of a vortex line element is written as [3]:

$$\mathbf{u} = \frac{\Gamma}{4\pi}\kappa\left(\ln\frac{2L}{\varepsilon} - 1\right)\mathbf{b}, \tag{1}$$

where Γ is the vortex filament intensity, κ is the curvature, $2L$ is the length of a local segment, ε is the vortex filament radius, $\mathbf{b}$ is the binormal unit vector. LIA is true if the line cross-section is much smaller than the local curvature radius and there is no interaction between various parts of the vortex line. When the $(\Gamma/4\pi)(\ln 2L/\varepsilon - 1)$ factor is introduced into the time scale and the Frenet equations are accounted for, LIE can be written in a compact form

$$\frac{\partial \mathbf{X}}{\partial t} = \mathbf{X}' \times \mathbf{X}''. \tag{2}$$

Here, $\mathbf{X}$ is a radius vector of a point on a vortex filament; the prime means a derivative with respect to an arc position. In [7], a transformation is proposed that brings equation (2) to the nonlinear Schrödinger equation

$$i\frac{\partial \psi}{\partial t} + \psi'' + 2|\psi|^2\psi = 0, \tag{3}$$

where the complex function ψ is related to the torsion τ and curvature κ of the vortex filament as

$$\psi = \frac{1}{2}\kappa\exp\left(i\int_0^s \tau\, ds - \frac{i}{2}\int_0^t A(t)dt\right). \tag{4}$$

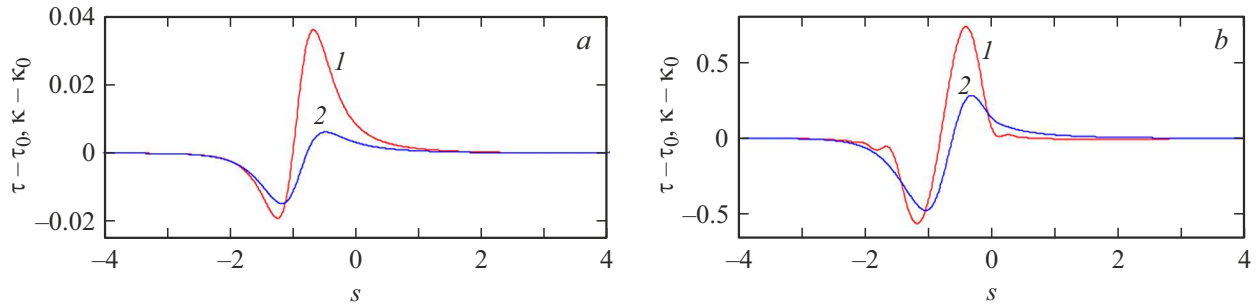

Figure 1. Deviation of the torsion (*1*) and curvature (*2*) from the initial dependences at $t = 0.001$ (*a*) and 0.035 (*b*).

Here, s is the arc coordinate, $A(t)$ is an arbitrary time function that can be taken as zero.

This work provides numerical solution to equation (3) with an initial condition corresponding to a conical helical vortex, whose geometry is set as in [11]:

$$x = r_0(z)\cos(\lambda z),\ y = r_0(z)\sin(\lambda z),$$
$$r_0(z) = [1 + \tanh(kz)]/2. \qquad (5)$$

Equations (5) represent smooth cross-linking of a semi-infinite straight-lined vortex with a semi-infinite cylindrical helical vortex (helix radius is taken equal to 1, thus, the length scale is assigned). $2\pi/\lambda$ is the helix pitch, k characterizes the rate of radius change from 0 to 1 and is responsible for the helical vortex cone angle.

Arc coordinate for a curve defined by equations (5) takes the form of an integral

$$s = \int_0^z \sqrt{\left(\frac{\partial x}{\partial z}\right)^2 + \left(\frac{\partial y}{\partial z}\right)^2 + 1}\, dz = \frac{1}{2k}\int_{0.5}^{r_0(z)} \frac{\sqrt{q(r)}}{r(1-r)} dr,$$
$$q(r) = \left[4k^2(1-r)^2 + \lambda^2\right] r^2 + 1. \qquad (6)$$

Corresponding expressions for initial dependences of curvature and torsion on r_0 are written as

$$\kappa_0(r_0) = q(r_0)^{-1}$$
$$\times\sqrt{r_0^2\lambda^4 + 4k^2\left[(1-2r_0)^2 + r_0^2\lambda^2 - \left(1 - 2r_0 - r_0^3\lambda^2\right)^2 q(r_0)^{-1}\right]},$$
$$\tau_0(r_0) = \lambda r_0^2\left[16k^4(1-r_0)^2 + 8k^2\lambda^2(1-r_0^2) + \lambda^4\right]$$
$$\times q(r_0)^{-3}\kappa_0(r_0)^{-2}. \qquad (7)$$

When r_0 is small, the curvature and torsion have the asymptotes $(4k^2 + \lambda^2)r_0$ and λ, respectively, and when $r_0 \to 1$, we have the asymptotes $\lambda^2/(1+\lambda^2)$ and $\lambda/(1+\lambda^2)$, which coincide with the curvature and torsion of the classical helical vortex.

Arc coordinate s is a variable in equation (3). To find the initial dependence $\psi_0(s)$, we proceed to s in equations (7), for which $r_{s0}(s)$ shall be implicitly assigned through integral (6). Here, it is reasonable to use the Newton method because the derivative dr_{s0}/ds is described by a simple function $dr_{s0}/ds = 2kr_{s0}(1-r_{s0})/\sqrt{q(r_{s0})}$, and $r_0(s + 0.342)$ at $s < -0.219$ and $r_0\left[(s + 0.626)/\sqrt{1+\lambda^2}\right]$ at $s \geqslant -0.219$ can be taken as the initial approximation. These dependences are the asymptotes $r_{s0}(s)$ at $s \to -\infty$ and $s \to \infty$, respectively. It should be noted that $r_{s0}(0) = 0.5$.

As the boundary conditions for equation (3), we require that the values of ψ and its derivative ψ' coincide with ψ_0 and ψ_0', respectively, at $s \to \pm\infty$.

For numerical solution of equation (3), we use a method of finite differences. For this, we choose an interval of integration with respect to s. Analysis shows that the interval $[-10, 10]$ is sufficient for investigating the vortex behavior with moderate values of k and λ (see the discussion below). We break the interval by a uniform grid with the step Δs and use the central differences for approximation ψ''. Time integration is performed using an explicit scheme.

Calculations give $\psi(s)$ at each time step. As we are interested in the curvature and torsion, in accordance with equation (4), we have

$$\kappa(s,t) = 2\left|\psi(s,t)\right|, \quad \tau(s,t) = \frac{\partial}{\partial s}\mathrm{Im}\left[\ln\left(\psi(s,t)\right)\right]. \qquad (8)$$

Evolution of a vortex filament with $k = 1.5$, $\lambda = \pi$ is discussed as an example. An arc coordinate step $\Delta s = 0.01$ and time step $\Delta t = 10^{-7}$ were chosen for calculation. Explicit scheme provides adequate results only at a finite time interval with small Δt. Therefore, a step for calculation was chosen empirically where the same result was obtained with twice as small step. With short times, vortex behavior can be easily observed by considering the torsion and curvature deviation from initial dependences: $\tau(s,t) - \tau_0(s)$, $\kappa(s,t) - \kappa_0(s)$. Figure 1, *a* shows deviations at $t = 0.001$. The torsion deviation amplitude is much higher than the curvature deviation amplitude; then focus is made on the torsion behavior. Single perturbation with its center at $s = -0.585$ with $\Lambda = 1.026$ is formed at the initial stage. With time, the wave amplitude and wavelength increase, while the perturbation center moves to the right. At $t = 0.035$ (Figure 1, *b*), two new waves are initiated on the left ($s = -1.740$) and on the right ($s = 0.260$).

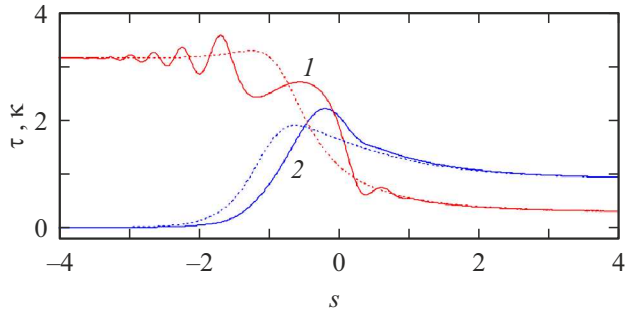

Figure 2. Torsion profile (*1*) and curvature profile (*2*) at $t = 0$ (dashed lines) and 0.06 (solid lines).

By time $t = 0.06$ shown in Figure 2, waves appear directly on $\tau(s,t)$ and $\kappa(s,t)$. Initial torsion and curvature profiles are shown by dot lines. There are many waves in the region of negative s, whereas the wave amplitude and wavelength decrease as the position moves away from zero. The first wave at $s > 0$ is the most interesting one in terms of formation of configuration preceding the vortex reconnection. Here, torsion starts approaching zero. With negative s, as the wave amplitude grows, the torsion can also take small values, but the curvature here is small, i. e. the vortex is almost straight-lined and the probability of reconnection is low. The first torsion minimum at $s > 0$ further decreases linearly with time (Figure 3, *a*), and the wave amplitude grows. Wave motion (local torsion minimum and maximum positions) is reflected in Figure 3, *b*. $\Lambda = 2(s_{\max} - s_{\min})$ grows and wave propagation velocity decreases. At $t = 0.0956$, the torsion minimum reaches zero at a point with $s = 0.691$. Zero torsion corresponds to the experimental data [1], at which a pre-reconnection vortex loop is formed. Interval of NSE integration with respect to the angular position $[-10, 10]$ was specified above. Preliminary calculations within $[-5, 5]$ have shown that a selected wave was formed when zero torsion was reached in the same position and at the same time, but with negative s, wave propagation caused violation of the boundary condition. Increase in the integration interval allowed this problem to be solved.

This work proposes an approach to simulation of conical helical vortex filament behavior via numerical solution of the nonlinear Schrödinger equation. Solution was sought for in curvature–torsion variables. The study has found wave-like behavior of curvature and torsion caused by the initial vortex form. A specific wave is pointed out, evolution of which induces a region with zero torsion, which corresponds to the appearance of a loop on a vortex filament preceding the vortex reconnection.

The discussed vortex filament geometry is qualitatively close to that observed in the experiment [1] and in a system, which more accurately simulated the hydraulic turbine flow path [12]. However, both the helix pitch and cone angle of the conical helical vortex may vary depending on the model geometry and swirling in the experiment (or on the system geometry and mode of operation in the hydraulic turbine case). Dependence of vortex behavior (and possibility of situation where the torsion decreases to zero) on selection of k and λ shall be identified, and dependences, which better describe the observed vortex forms in real equipment, shall be sought for.

The findings are important for the development of theoretical approaches to description of the self-reconnection phenomenon in the conical helical vortex, which has been found experimentally [1]. These approaches can be, in particular, used for understanding the causes of heavy aperiodic impacts in the flow downstream of the hydraulic turbine runner.

Conflict of interest

The author declares no conflict of interest.

References

[1] S.V. Alekseenko, P.A. Kuibin, S.I. Shtork, S.G. Skripkin, M.A. Tsoy, JETP Lett., **103** (7), 455 (2016). DOI: 10.1134/S002136401607002X
[2] R. Ricca, Nature, **352**, 561 (1991). DOI: 10.1038/352561a0
[3] L.S. Da Rios, Rend. Circ. Mat. Palermo, **22**, 117 (1906). DOI: 10.1007/BF03018608
[4] F.R. Hama, Phys. Fluids, **5**, 1156 (1962). DOI: 10.1063/1.1706500

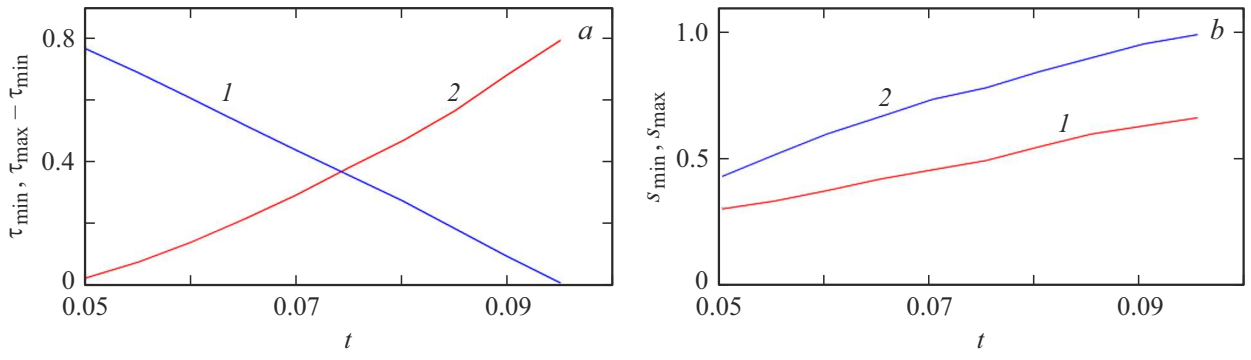

Figure 3. Behavior of the properties of the first torsion wave at $s > 0$. *a* — local minimum (*1*) and wave span (*2*); *b* — positions of the local minimum (*1*) and maximum (*2*).

[5] R.J. Arms, F.R. Hama, Phys. Fluids, **8**, 553 (1965). DOI: 10.1063/1.1761268
[6] R. Betchov, J. Fluid Mech., **22**, 471 (1965). DOI: 10.1017/S0022112065000915
[7] H. Hasimoto, J. Fluid Mech., **51**, 477 (1972). DOI: 10.1017/S0022112072002307
[8] J. Cieśliński, Phys. Lett. A, **171**, 323 (1992). DOI: 10.1016/0375-9601(92)90651-2
[9] Y. Fukumoto, T. Miyazaki, J. Phys. Soc. Jpn., **55**, 4152 (1986). DOI: 10.1143/JPSJ.55.4152
[10] H. Salman, Phys. Rev. Lett., **111**, 165301 (2013). DOI: 10.1103/PhysRevLett.111.165301
[11] P.A. Kuibin, E3S Web Conf., **592**, 02010 (2024). DOI: 10.1051/e3sconf/202459202010
[12] G.D. Ciocan, M.S. Iliescu, in *Proc. of 24th Symp. on hydraulic machinery and systems* (Foz do Iguassu, Brasil, 2008). https://www.researchgate.net/publication/235331921_3D_PIV_Measurements_in_Two_Phase_Flow_and_Rope_Parametrical_Modeling

Translated by E.Ilyinskaya